Characterization and utilization of *Sargassum linifolium* and *Stypopodium schimperi* polysaccharides as blue inhibitors for steel electo-polishing

Abeer A. M. El-Sayed, F. M. Abouzeid, Mona M. Ismail and Gehan M. ElZokm

ABSTRACT

Different polysaccharide extracts (crude polysaccharide, fucoidan and alginate) from *Sargassum linifolium* and *Stypopodium schimperi* were examined as inhibitors of the carbon steel anodic dissolution process in 8 M phosphoric acid. The anode potential and limiting current relationship was measured and compared for gradually increasing algae extract concentrations (from 20 to 350 ppm). The limiting current decreases while inhibition efficiency (%) increases as the concentrations of all these extracts increase. Fucoidan from *S. linifolium* is considered to have the most retardation effect. The extracts' retardation mechanism is depending on the adsorption process at the steel metal, which was proved by scanning electron microscopy (SEM). Also, SEM shows that high concentration (350 ppm) of *Stypopodium schimperi* crude polysaccharide, *Sargassum linifolium* fucoidan and *Stypopodium schimperi* alginate extracts have promising effect on the surface texture. The data of Langmuir and the kinetic–thermodynamic isotherms were determined to clarify the nature of adsorption of extract on the metal–solution interface. The activation energy and activation parameters (changes in enthalpy, entropy and Gibbs free energy) were determined and gave indication for strong interaction between the inhibitor and the steel surface. The extract features were investigated via Fourier transform infrared spectroscopy. The polysaccharides from the brown algae, especially fucoidan, manifest potential as a natural electro-polishing blue inhibitor. Surface morphology study confirmed that addition of algae extract to a steel dissolution bath enhanced the surface appearance and its texture quality to great extent.

Key words | adsorption isotherms, alginate, electro-polishing, fucoidan, macroalgae, steel

Abeer A. M. El-Sayed
Mona M. Ismail
Gehan M. ElZokm
National Institute of Oceanography and Fisheries,
Alexandria,
Egypt

F. M. Abouzeid (corresponding author)
Chemistry Department, Faculty of Science,
Alexandria University,
Alexandria,
Egypt
E-mail: *fatma.abouzeid@yahoo.com*

HIGHLIGHTS

- Extract of different polysaccharides (crude polysaccharide, fucoidan and alginate) under investigation used as blue inhibitor for electro-polishing of anodic carbon steel.
- Fucoidan is more inhibitory than the other two extracts owing to the chemical composition of fucoidan.
- Steel surface at high concentrations of different polysaccharides during anodic polishing became more smooth and bright, as confirmed by SEM.

INTRODUCTION

Brown marine macroalgae (Phaeophyta) represent a large group and they are the second most common group of seaweeds (Mestechkina & Shcherbukhin 2010). They play an important role in marine environments as very important resources of food, feed and energy and are rich sources of structurally diverse polysaccharides with valuable biological activities, which are not found in land plants (Ismail *et al.* 2017; Zhao *et al.* 2018; Wang *et al.* 2019). The brown algae produce polysaccharides such as fucoidan, alginate and laminarin. Polysaccharides are bio-macromolecules of

doi: 10.2166/wst.2020.586

monosaccharide units joined together via glycosidic bonds and they have different applications in industry as stabilizers, thickeners and food; also, they have bioactive features as anti-cancer and anti-inflammatory activities (Wang *et al.* 2019). Seaweed polysaccharides are various, according to the algae species, the extraction process, season of harvest and local climatic conditions.

Fucoidan is a branched polysaccharide sulfate ester of the family of sulfated homo- and hetero-polysaccharides. The main monomer in fucoidan is fucose, with a simple structure as shown in Figure 1(a) (Fletcher *et al.* 2017). Fucoidan is composed of two chain structures, one with $(1 \rightarrow 3)$-α-L-fucopyranose as the chain and the other with α-L-fucopyranose linked by $(1 \rightarrow 3)$ and $(1 \rightarrow 4)$ as the main chain. Single and double substitutions in the sulfate groups at the C-2 or C-4 positions of both skeletons can occur. Some fucoidans possess substituted branches at the C-2 and C-3 positions (Ale *et al.* 2011). It also contains galactose, mannose, xylose and glucuronic acid residues (Bilan *et al.* 2010). Fucoidan is a nontoxic polyelectrolyte that possesses various pharmacological activities, i.e. antioxidant, antibacterial, antiviral, antitumor and anticoagulant activities.

Alginate is the main structural polysaccharide existing in brown seaweeds; it consists of β-D-mannuronate (M) and α-L-guluronate (G) units (Figure 1(b)), linked together in different sequences as MM (β-D-mannuronate–β-D-mannuronate) or GG (α-L-guluronate–α-L-guluronate) or MG (β-D-mannuronate–α-L-guluronate) or GM (α-L-guluronate–β-D-mannuronate) (Rioux *et al.* 2007). Alginate is widely used in textile printing, paper coating and other relatively industrial applications because of its ability to retain water and its gelling, viscosifying and stabilizing properties. Further, these compounds are utilized as blue polymer inhibitors that protect metal electrodes from dissolution during steel electro-polishing.

Electro-polishing is an electrochemical process that polishes a metal surface in presence of an electrolyte solution via passage of electric current; it is also known as electrochemical polishing or electrolytic polishing or anodic polishing (Abouzeid & Abubshait 2020). The polishing rate depends on the limiting current value. The polishing phenomenon has a great importance in pharmacy; steel is widely used in many kinds of industries such as chemical, medical, textile and paper, and also in biomaterials, surgical and petroleum refining apparatus.

It is generally accepted that organic molecules retard dissolution via adsorption at the metal–solution interface (Hassan 2007). Where two primary mechanisms of chemical or physical adsorption are associated with organic compounds, they act firstly by blocking the reaction sites or generating a physical barrier to reduce the diffusion of dissolved species to the metal surface, since the adsorption is dependent on the following factors:

– additives concentration
– electrochemical potential at the interface.

One patent of 1958 used commercial alginate in the process of electro-polishing (Robinson 1958). There are no studies using crude polysaccharides, fucoidan and alginate extracted from brown marine algae in the electro-polishing of steel, as in the present study.

Recently algae extracts have been used as dissolution inhibitors (Benabbouha *et al.* 2018). These authors investigated the effect of isopropanol extract of a red alga, *Halopitys incurvus*, on carbon steel in 1 M HCl, obtaining a maximal value of inhibition efficiency of 81.86% at 600 mg L^{-1} at 298 K. Benabbouha *et al.* (2020) investigated the isopropanol extract of brown seaweed *Cystoseira baccata*, against corrosion of carbon steel in 1 M HCl, with maximal value of inhibition efficiency of 86.5% obtained at 700 mg L^{-} at 298 K. Verma & Khan (2016) investigated the isopropanol extract of green algae *Spirogyra*, against corrosion of carbon steel in 0.5 M HCl, with maximal value of inhibition efficiency of 93.03% at 2 g L^{-1}. Ramdani *et al.* (2015) investigated a marine macroalgae extract of *Caulerpa prolifera*, against corrosion of mild

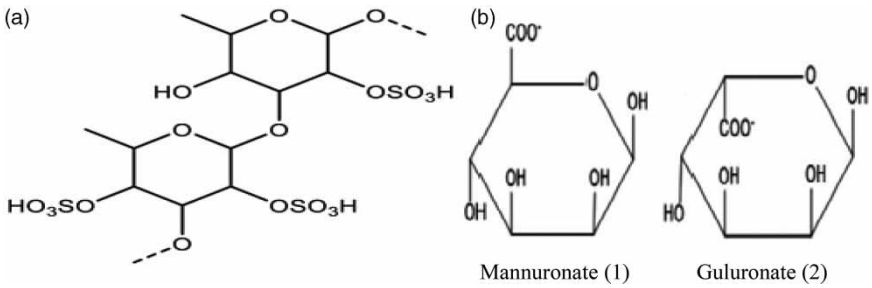

Figure 1 | The typical configuration of the main polysaccharides of brown seaweeds. (a) Fucoidan structure, (b) structure of alginate: mannuronate (1) and guluronate (2).

steel in 1 M HCl, with maximal value of inhibition efficiency of 94.95% at 1 g L^{-1}.

The use of algae extracts for the retardation of the metal dissolution has some advantages over the use of some organic/inorganic inhibitors because they are nontoxic, cheap, and environmentally friendly. They can be easily produced and purified. Generally many authors agree that algae extracts are inhibitors that can compete favorably with green corrosion inhibitors.

The current work is devoted to extraction and characterization of crude polysaccharides, fucoidan and alginate (Figure 1) from two brown seaweeds *Stypopodium schimperi* and *Sargassum linifolium*. The work also aims to use these different polysaccharides as blue inhibitors for steel electrolytic polishing and investigates the optimum concentrations, temperature, activation parameters and adsorption isotherms of these different polysaccharides; also the resulting surface morphology is investigated by scanning electron microscopy (SEM).

MATERIALS AND EXPERIMENTAL METHODS

Collection and identification of seaweeds

The marine algae *Sargassum linifolium* C.Agardh and *Stypopodium schimperi* (Kützing) Verlaque & Boudouresque (Figure 2) used for this study were freshly collected from Hurghada coast along the Red Sea, Egypt. A portion of the seaweeds was processed as herbarium specimens on the same day of collection; *Sargassum linifolium:* thalli up to 25–30 cm high, filamentous, while the thallus length of *Stypopodium schimperi* was 17–20 cm. As shown in Figure 2, whole thalli of the collected seaweed were processed as herbarium sheet and were preserved in the Taxonomy and Biodiversity Laboratory of Aquatic Biota. Other portions were preserved in 5% formalin in sea water for taxonomic classification. The remaining cleaned seaweeds were air-dried in the shade at room temperature for several days, and then were finally powdered and stored at −20 °C until used. All seaweeds were identified taxonomically following the Kanaan method (Kanaan & Belous 2016). The names of the species were used according to Guiry & Guiry (2019) and were confirmed using Algae Base website.

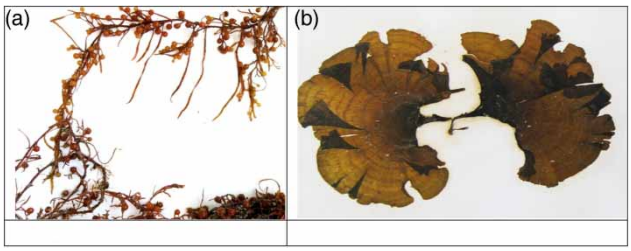

Figure 2 | Photos of the tested seaweeds: (a) *Sargassum linifolium* and (b) *Stypopodium schimperi.*

Extraction of different polysaccharides

The extraction of soluble polysaccharides was described by El-Rafie *et al.* (2013). Fucoidan was extracted via the following method (Preeprame *et al.* 2001) with some modifications. The extraction process ran for 12 hrs at 25 °C, while the original Preeprame *et al.* method extraction process occurred at boiling temperature for 1 hr.

The alginate extraction was developed according to the method of Haug *et al.* (1974). The yield of extraction was determined by Equation (1) as percentage/dry weight (AOAC 1990):

$$\text{Yield of extract} = \frac{\text{weight of extract}}{\text{dry weight}} \times 100 \quad (1)$$

dry weight = weight of seaweed that is the source of crude polysaccharides.

Moisture content of these extracted samples was determined according to the standard AOAC method (AOAC 2000). Sulfate content was measured according to the turbidimetric method (APHA *et al.* 1999).

Fourier transform infrared spectroscopy (FT-IR)

The extracted samples were distinguished utilizing FT-IR in a Burcker Optik GmbH Model No.-Tensor 27 using KBr pellet technique in the frequency range of 200–5,000 cm^{-1}.

Surface study (SEM)

A JEOL JSM-5300 scanning microscope, Oxford, UK, was used to examine the surface topography of the specimens. The steel specimen was 1 cm ×1 cm.

The electrolytic cell and electrical circuit of electropolishing

The cell used in the natural convection (Figure 3) consisted of a rectangular Plexiglass container with a base of 15 × 5 cm and a height of 10 cm with electrodes fitting the whole

Figure 3 | Electrical cell.

cross-section. The electrodes were rectangular C-steel sheets of 10 cm height and 5 cm width. The components of steel sheet were Fe, S, P, Mn and C with 99.4043, 0.0257, 0.07, 0.4 and 0.1%, respectively. Electrode separation was 15 cm. Before each run the cell was filled with 8 M H_3PO_4 solution and the active height of the anode was adjusted by insulating the rest of the anode by epoxy resin on the inactive part. Active anode height was 2 cm while the cathode height was fixed at 5 cm. The electrical circuit consisted of a 6 V DC power supply, a variable resistance and a multirange ammeter connected in a series with the cell. A high impedance voltammeter was connected in parallel with the cell to measure its potential. The steady-state anode potential was measured against a reference electrode consisting of a small steel sheet immersed in a cup of luggin tube filled with H_3PO_4-natural products solution similar to that in the cell. The tip of the luggin tube was placed 0.5–1 mm from the anode wall. Polarization curves, from which the limiting current (I_L) was determined, were plotted by increasing the applied current stepwise and measuring the corresponding steady-state anode potential. Two minutes were allowed for reaching the steady-state potential. Before each run, the back of the anode was insulated with polystyrene lacquer and the active surface was polished with fine emery paper, degreased with trichloroethylene, washed with alcohol and finally rinsed in distilled water. The temperature was regulated by placing the cell in a thermostatic water bath at different temperatures (20, 30, 40 and 50 °C) ± 1 °C. The reproducibility of the limiting current with concentration (polarization curve) was confirmed via carrying out at least three separate trials.

RESULT AND DISCUSSION

The percentage yield of different polysaccharides

The percentage yield of polysaccharides, fucoidan and alginates from *Sargassum linifolium* and *Stypopodium schimperi* is shown in Table 1 and Figure 4. The total yield of crude polysaccharides ranged from 1.48 to 10.35% for *S. linifolium* and *St. schimperi*, respectively. These values were in good agreement with reports of earlier studies (Berteau & Mulloy 2003) but were lower than recorded in *S. naozhouense* (21.01%). The yield of fucoidan extracts of *S. linifolium* (13.04%) was higher than in *St. schimperi* (9.085%); this may be related to the morphological form of *S. linifolium*, which has three leaves, whereas *St. schimperi* has two, which are sheet-like with no stem (Figure 2). These results were in good agreement with other results. Although there are clear links between algal species and fucoidan structure, there is insufficient evidence so far to establish any systematic correspondence between sugar composition and algal order. Also, the variation in the fucoidan content from brown seaweeds may be related to their species, seasons and locations as demonstrated previously (Zvyagintseva & Mel'nikov 2012).

On the other hand, *St. schimperi* contained higher concentrations of alginate (48.68%) as compared with *S. linifolium* (43.41%). Our results were in agreement with Draget *et al.* (2006) who demonstrated that alginate accounts for up to 40% of the *Sargassum* spp., *Macrocystis* spp., *Ascophyllum* spp. and Fucales species dry matter. The alginate yield of both tested seaweeds was higher than

Table 1 | Percentage yield, moisture (%) and sulfate content (mg g^{-1}) of polysaccharides, fucoidan and alginate from the tested brown seaweeds

	Crude polysaccharides			Fucoidan			Alginate		
Algal spp.	**Yield**	**Moisture**	**Sulfate**	**Yield**	**Moisture**	**Sulfate**	**Yield**	**Moisture**	**Sulfate**
Sargassum linifolium	1.48	0.056	263.23	13.04	0.582	316.96	43.41	1.63	25.23
Stypopodium schimperi	10.35	0.403	286.56	9.085	0.328	357.96	48.68	1.43	33.56

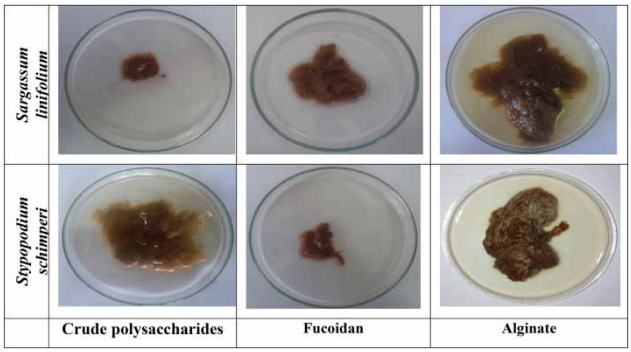

Figure 4 | Different extracts of polysaccharides.

the yield of *S. sinicola* (5.7 ± 0.2%) which was collected from Bahía de La Paz, Baja California Sur, Mexico (Rodríguez-Montesinos *et al.* 2008).

From Table 1, the highest yield from each extracted polysaccharide with maximum sulfate content was selected to evaluate them as natural inhibitors in anodic polished stainless steel.

Moreover, Paniagua-Michel *et al.* (2014) recorded that the crude polysaccharide concentrations in the seaweed species represent up to 4–76% of their dry weight. *Sargassum wightii* showed maximum yield of polysaccharide (15.64%), followed by *Padina* sp. (15.16%) and *Dictyota* sp. (7.4%) (Jayaraman *et al.* 2016). Sulfate content in *Lessonia nigrescens* crude polysaccharides fluctuated in the range 33.7–40.5% depending on extraction method and their fraction (Zou *et al.* 2019). Total yield of the fucoidans obtained from brown alga *Fucus vesiculosus* ranged from 2.8 to 3.4%, while the yield of fucoidan from *Ascophyllum nodosum* was from 2.6 to 4.1% (Kim 2012). The sulfate content of fucoidan from brown algae *F. vesiculosis and A. nodosum* ranged between 35 and 40% of the fucoidan (Kloareg *et al.* 1986). Fucoidan extracted from ncomplte sentence *L. vadosa* contained 37.7% sulfate (Nancy *et al.* 2004). The fucoidan from *Sargassum hornei* contained about 26–28.6% of sulfate (Kimura *et al.* 2007). About 17.7% of alginate was extracted from *Sargassum latifolium* (Larsen *et al.* 2003). Kim *et al.* (2011) reported that alginate represents up to 40% of dry weight of most brown seaweed.

FT-IR spectrum of different polysaccharides

Crude polysaccharide

The FT-IR spectrum indicated that the crude polysaccharide of the two tested seaweeds possessed similar characteristic peaks (Figure 5(a)). Briefly, the wide peak at 3,418 and 3,378 cm^{-1} and a small peak at 2,933 and 2,937 cm^{-1} are due to the stretching vibrations of O–H and C–H for *St. schimperi* and *S. linifolium*, respectively. The bands at 2,931 and 2,933 cm^{-1} can be attributed to the alkane C-H stretching or assigned to the secondary amine. The sharp bands at 1,621 and 1,644 cm^{-1} were attributed to carboxylate O–C–O asymmetric stretching or can be assigned to the amide groups of protein or to the carbonyl stretching groups of *St. schimperi* and *S. linifolium* polysaccharides, respectively (Kannan 2014). The peaks at 1,431 and 1,427 cm^{-1} indicated C-H bending vibration of polysaccharide composed of D-glucose, D-mannose, D-xylose and galacturonic acid for *St. schimperi* and *S. linifolium*,

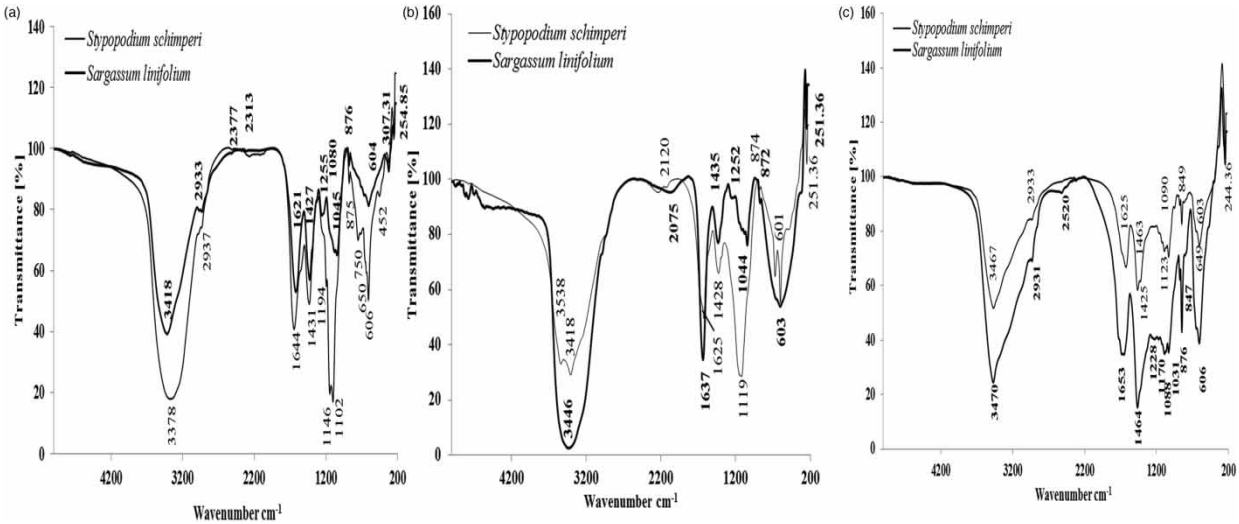

Figure 5 | FT-IR spectrum of the tested brown seaweeds for (a) crude polysaccharide, (b) fucoidan and (c) alginate.

respectively or assigned to COO group in alginate (Kannan 2014). The spectrum of *S. linifolium* polysaccharide contained a short peak at 1,255 cm^{-1} which was due to the presence of sulfated ester groups (S=O), which is a characteristic component in fucoidan, and at 1,045 and 1,080 cm^{-1} which corresponded to the S=O stretch of the sulfated polysaccharides or the C-N stretching of aromatic amine group, whereas the band at 1,102 cm^{-1} in *St. schimperi* polysaccharides is allocated to C-O groups of polyols of polysaccharides (Chandía & Matsuhiro 2008). A very strong band for both algae, characteristic for asymmetric stretching vibrations of the RO–SO_3- bond of the sulfate groups, is found approximately in the range 1,146–1,020 cm^{-1}. This band is slightly split, reflecting inner-sphere complexes (largely covalent in character). The bands in tested seaweeds at 875–876 cm^{-1} are assigned to C-O-SO_4 of sulfated polysaccharides (Besednova *et al.* 2010; Kannan 2014). All these suggested that the polysaccharide of both tested seaweeds may be fucoidan and alginate.

Fucoidan

On the basis of FT-IR analyses, although fucoidan spectra of tested brown seaweeds were similar, some differences in minor peak patterns were observed (Figure 5(b)). A broad band at 3,446 cm^{-1}, assigned to the OH stretching vibrations, indicated the presence of moisture in the sample, as H_2O contains O-H bonds that give a stretching vibration signal (Silverstein & Webster 1998). A sharp intense band observed at 1,637 & 1,625 cm^{-1} can be due to amide-I group, which is mainly related to stretching vibration mode of C=O (Pereira *et al.* 2003) and bands at 1,435 & 1,428 cm^{-1} were attributed to the presence of the asymmetrical bending vibration of CH_3 for *S. linifolium* & *St. schimperi*, respectively. The absorption at 1,252 cm^{-1} of *S. linifolium* spectrum indicated sulfated ester groups (S=O) which are a characteristic component in fucoidan (Silverstein & Webster1998). A very sharp band recorded at 1,119 cm^{-1} for *St. schimperi* represented RO–SO_3-. It is noteworthy that an absorption small band at around 1,044 cm^{-1} assigned to the SO_3 group in fucoidan was detected only for *S. linifolium*. The spectrum of *St. schimperi* and *S. linifolium* showed a band at 872 and 874 cm^{-1}, respectively, assigned to the C-H deformation vibration of b-mannuronic acid residues (Pereira *et al.* 2003) or pointing to C-O-SO_4 of fucoidan. The band at 601 and 603 cm^{-1} for *St. schimperi* and *S. linifolium* may be due to C=C-H stretching vibration. Therefore, the presence of SO_3, CH_3 and OH groups as well as C-O-S bonds enabled us to identify the extraction polysaccharide from two species as fucoidan (Lim *et al.* 2014).

Alginate

Figure 5(c) shows the FT-IR spectra of the alginate extracted from *St. schimperi* and *S.linifolium*. The broad intense bands at 3,467 and 3,470 cm^{-1} are assigned to the OH group of the alginate polysaccharides (El-Rafie *et al.* 2013). The bands at 2,931 and 2,933 cm^{-1} can be attributed to the alkane C-H stretching or assigned to the secondary amine (El-Rafie *et al.* 2013). The bands 1,625 cm^{-1} in *St. schimperi* and 1,653 cm^{-1} in *S. linifolium* related to carbonyl (C=O) group in alginate. The bands appearing at 1,463 and 1,425 cm^{-1} in *St. schimperi* and 1,464 cm^{-1} in *S. linifolium* are assigned to carboxyl (COOH) group present in the alginate (Sheng *et al.* 2004). The short band at 1,228 cm^{-1} can be assigned to the C-O stretching vibration in *S. linifolium*, Bands at approximately 1,088–1,090 and 1,031 cm^{-1} in both species correspond to mannuronic (M) and guluronic (G) units respectively, as observed by Pereira *et al.* (2003) The bands at 1,123 cm^{-1} in *St. schimperi*, 1,170 cm^{-1} in *S. linifolium* and 1,088–1,090 cm^{-1} in both tested algae correspond to C-O and C-C-H groups, respectively present in mannuronic and guluronic acids forming the alginate. Multiple very small peaks observed in the range 1,050 and 1,250 cm^{-1} may be due to a bidentate binuclear (bridging) surface complex (Nakamoto 1986). The band at 1,031 cm^{-1} is attributed to alcohol groups in the alginate. The bands identified for mannuronic acid were at 849 cm^{-1} in *St. schimperi* and at 876 and 847 cm^{-1} in alginate of *S. linifolium*. Three bands (649 and 603 cm^{-1} in *St. schimperi* and 606 cm^{-1} in *S. linifolium)* are related to vibration of the glycosidic bond (C-O-C) (Campos-Vallette *et al.* 2010).

Leveling process (electro-polishing in H_3PO_4)

A typical polarization curve is obtained for an electrolyte consisting of orthophosphoric acid of concentrations ranging from 6 M to 14 M (Table 2). The curve (Figure 6) is divided into three parts, which are electrolytic etching, polishing and gas (O_2) evolution with pitting. The influence of H_3PO_4 concentration on the limiting current (I_L) values can be clarified based on the mass transfer Equation (2) (Taha *et al.* 2013a, 2013b).

$$I_L = \frac{nZFD}{\delta} C_{Fe3+} \quad (2)$$

Table 2 | H_3PO_4 concentration effect on the C-steel anodic dissolution at 20 °C

H_3PO_4 conc. (mol L^{-1})	I_L (A)	$10^3C^3_{Fe}$ (mol cm^{-3})	10^6D (cm^2 sec^{-1})	η (gm cm^{-1} sec^{-1})
6	0.52	1.00	4.15	1.891
8	0.45	0.99	3.61	4.211
10	0.31	0.82	3.35	5.750
12	0.26	0.80	1.03	6.220
14	0.07	0.76	0.93	14.35

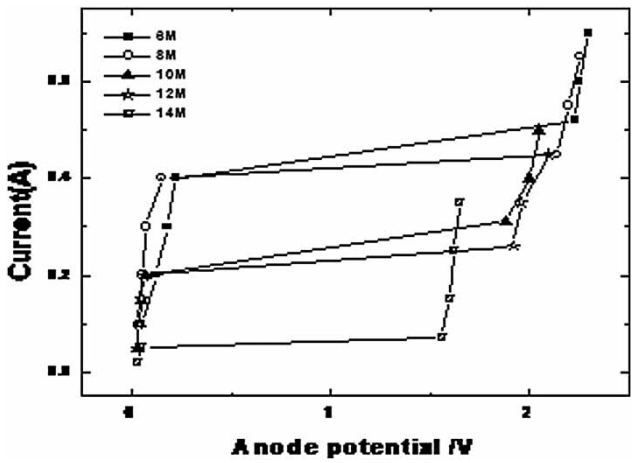

Figure 6 | Polarization curve for vertical C-steel plate electro-dissolution at 20 °C in the presence of different H_3PO_4 concentrations.

where I_L = limiting current (A); Z = working area (cm^2); n = charge of the ion involved; F = Faraday constant (C mol^{-1}); D = diffusion coefficient of the rate-limiting species (cm^2 s^{-1}); C_{Fe3+} = saturation concentration of iron (mol L^{-1}) of metal ions (Fe^{3+}) in the solution for the salt film mechanism or bulk C of the acceptor species for acceptor mechanism; and δ = thickness of the Nernst diffusion layer (cm).

The saturation solubility of $FePO_4$ decreases as H_3PO_4 concentration increases (Table 2) resulting in reduction in I_L. Also, increasing H_3PO_4 concentration leads to increase in solution viscosity (η) so diffusivity of Fe^{3+} ion (D) will decrease and diffusion layer thickness (δ) will increase resulting in reduction in I_L values. The limiting current performance through electro-polishing of C-steel in H_3PO_4 (Figure 6) is owing to the certainty that metal dissolution is controlled by mass transport (Abouzeid 2016) during the process; reaction products diffusion is limited and is considered as the rate-determining step of overall reaction rate. The mechanism of precipitated salt film engages diffusion rate limiting of dissolving metal cations from the anode surface into solution bulk (Taha *et al.* 2020). At the I_L value, a saturated concentration of metallic cation thin salt film is present on the surface of the anode and determines the rate at which metal ions depart the anode surface.

Structure effect of different polysaccharides

The influence of different polysaccharide extracts from tested seaweeds on the values of I_L, which determines the electro-polishing rate, has been investigated from the anodic polarization curves for carbon steel at 8 M H_3PO_4 and 20 °C. Figure 7 shows the anodic polarization curves in absence and presence of various concentrations

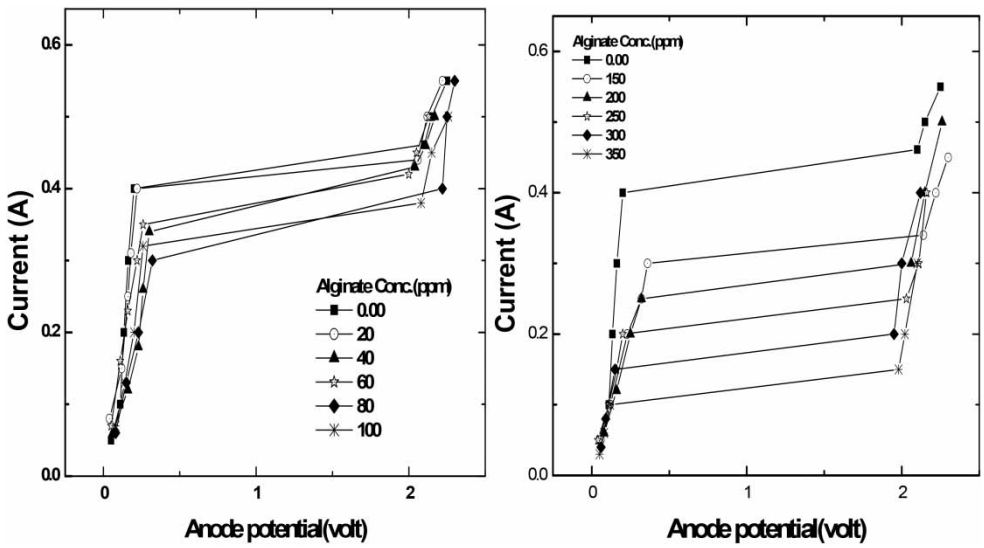

Figure 7 | The anodic polarization curves in absence and presence of various concentrations of alginate at 20 °C.

Table 3 | Values of limiting current (I_L) and inhibition efficiency percentage (IE%) for electro-polishing of steel in 8 M H_3PO_4 in the absence and presence of different polysaccharide extract at different temperatures

	20 °C		30 °C		40 °C		50 °C	
Conc. (ppm)	**I_L (A)**	**IE%**	**I_L (A)**	**IE%**	**I_L (A)**	**IE%**	**I_L (A)**	**IE%**
Polysaccharide								
0	0.461	–	0.505	-	0.562	–	0.612	–
20	0.422	8.46	0.463	8.32	0.52	7.47	0.582	4.9
40	0.41	11.06	0.44	12.87	0.5	11.03	0.563	8.01
60	0.4	13.23	0.43	14.85	0.48	14.59	0.541	11.6
80	0.38	17.57	0.41	18.81	0.462	17.79	0.521	14.87
100	0.362	21.48	0.4381	13.25	0.443	21.17	0.5	18.3
150	0.331	28.2	0.365	27.72	0.403	28.29	0.481	21.41
200	0.291	36.88	0.342	32.28	0.362	35.59	0.441	27.94
250	0.245	46.85	0.3	40.59	0.345	38.61	0.4	34.64
300	0.185	59.87	0.25	50.5	0.3	46.62	0.35	42.81
350	0.135	70.72	0.2	60.4	0.242	56.94	0.3	50.98
Fucoidan								
0	0.461	–	0.505	–	0.562	–	0.612	–
20	0.4	13.23	0.453	10.3	0.51	9.25	0.562	8.17
40	0.39	15.4	0.43	14.85	0.5	11.03	0.544	11.11
60	0.38	17.57	0.41	18.81	0.475	15.48	0.525	14.22
80	0.37	19.74	0.4	20.79	0.46	18.15	0.5	18.3
100	0.342	25.81	0.381	24.55	0.433	22.95	0.488	20.26
150	0.3	34.92	0.345	31.68	0.393	30.07	0.466	23.86
200	0.288	37.53	0.312	38.22	0.355	36.83	0.425	30.56
250	0.222	51.84	0.28	44.55	0.325	42.17	0.386	36.93
300	0.162	64.86	0.244	51.68	0.289	48.58	0.35	42.81
350	0.12	73.97	0.185	63.37	0.233	58.54	0.285	53.43
Alginate								
0	0.461	–	0.505	–	0.562	–	0.612	–
20	0.443	3.9	0.483	4.36	0.532	5.34	0.6	1.96
40	0.431	6.51	0.466	7.72	0.515	8.36	0.582	4.9
60	0.421	8.68	0.448	11.29	0.5	11.03	0.562	8.17
80	0.4	13.23	0.423	16.24	0.482	14.23	0.551	9.97
100	0.382	17.14	0.4	20.79	0.463	17.62	0.535	12.58
150	0.342	25.81	0.383	24.16	0.423	24.73	0.492	19.61
200	0.304	34.06	0.352	30.3	0.392	30.25	0.452	26.14
250	0.253	45.12	0.312	38.22	0.355	36.83	0.416	32.03
300	0.2	56.62	0.267	47.13	0.319	43.24	0.367	40.03
350	0.153	66.81	0.218	56.83	0.267	52.49	0.322	47.39

of alginate for example, but polarization curves of other extracts are not shown. Table 3 gives the relation between I_L, percentage of inhibition efficiency (IE%) and different concentrations of different polysaccharide. It was found that the limiting current decreases with increasing the concentration of different extracted polysaccharides (addition of crude polysaccharide, fucoidan and alginate to electro-polishing bath led to retardation in electro-

polishing rate). It was found that values of IE% were dependent on the type of polysaccharides and their concentrations. IE% for the electro-polishing reaction is calculated from the relation (Taha *et al.* 2013a, 2013b):

$$IE\% = [(I_L)_o - (I_L)/(I_L)_o] \times 100 \quad (3)$$

where $(I_L)_o$ and (I_L) are the limiting current in absence and presence of different polysaccharides respectively.

Figure 8 shows the relation between IE% in the rate of the electro-polishing reaction and different concentrations of all polysaccharides at 8 M H_3PO_4 and 20 °C. It is observed that:

- the percentage inhibition efficiency increases as the concentrations of all these polysaccharides increase at all concentrations studied
- the order of extract inhibition is as follows: fucoidan > crude polysaccharide > alginate

It can be seen from Table 3 and Figure 8 that the anodic limiting current decreases as different polysaccharides concentrations increase at all concentrations studied (20–350 ppm) and IE% increases as the concentrations of all these polysaccharides increase; hence, the electro-polishing process of steel is decreased consequently. This may be attributed to the following facts.

- Adsorption of these additives on the steel anodic surface may form an adsorbed layer at the steel anodic surface; which leads to decrease in the diffusivity of Fe^{2+} ions and an increase in the resistance to the rate of mass transfer of Fe^{2+} from anode surface to bulk solution; hence, the rate of steel electro-polishing will be decreased. Also adsorption of the additives on the steel surface depends mainly on their structure (Abdel Rahman *et al.* 2015).
- Increase of solution viscosity in presence of these compounds reduces electric conductivity of Fe^{2+} ions; this led to a hindrance in flow of solution via the anodic surface, thus limiting current value decreases (Abdel Rahman *et al.* 2015).
- The chemical composition of fucoidan is different from that of other additives; it contains a large number of pyranoid units with polycentric adsorption positions (containing S and O atoms). These features would give the compound the following abilities: adsorption on the metal–solution interface through the electrostatic attraction between the charged metal and the charged inhibitor molecules, dipole-type interaction between unshared electron pairs in the compounds and the metal, π electron interaction with the metal, and integration of all of the above (Abouzeid 2016).
- The structure of fucoidan contains higher density of SO_3 and OH groups than other additives, that bind with iron ions. This gives the advantage to retard the aggressive attack of ions by acid and the dissolution of working electrode (Awad *et al.* 2010).
- The presence of sulfated ester groups S=O at the equatorial position of fucoidan maybe decreased the interaction between anode metal and acid medium through binding with metal ions (Abouzeid 2016). The glycosidic bonds between pyranoid rings and the hydrogen bonds formed with water molecules through the large numbers of hydroxyl groups in the case of fucoidan would require higher energy for the bonds to break, which leads to decrease in the mobility and the diffusivity of iron ions, with a consequent decrease in the rate of electro-polishing (Lim *et al.* 2014).

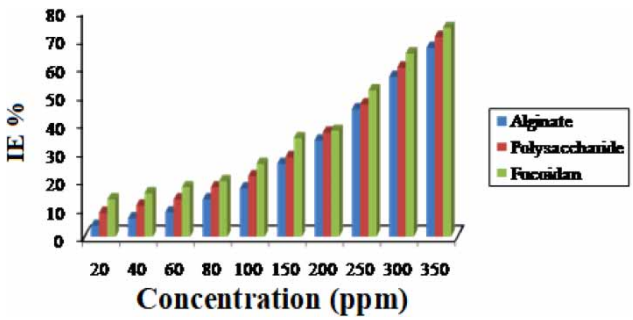

Figure 8 | Relation between IE% and concentrations of crude polysaccharide, fucoidan and alginate at 8 M H_3PO_4 and 20 °C.

Background of anodic dissolution mechanisms of iron

The mechanisms of active dissolution of iron (Figure 9) have been proposed in numerous papers, and they were summarized by (Vracar & Drazic 1992).

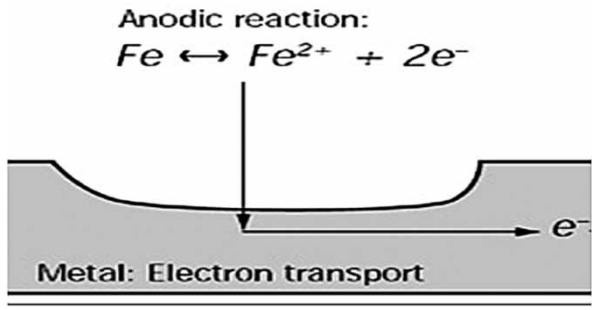

Figure 9 | Mechanisms of active iron dissolution.

As the first stage, FeOH(ads) forms and covers the surface.

From polarization measurements and reaction orders with respect to hydroxide ions (Allam *et al.* 1997), Heusler has proposed a catalytic mechanism:

$$Fe + OH^- = FeOH(ads) + e^{-e} \quad (4)$$

$$FeOH(ads) + Fe + OH^- = FeOH^+ + FeOH(ads) + 2e^- \quad (5)$$

$$FeOH^+ = Fe^{+2} + OH^- \quad (6)$$

The second step is catalytic and neither consumes nor produces the adsorption species.

In contrast Bockris & Reddy (2002) obtained kinetic data different from those of Heusler and proposed a catalytic consecutive-step (or non-catalyzed) mechanism:

$$Fe + OH^- = FeOH(ads) + e^- \quad (7)$$

$$FeOH(ads) = FeOH^+ + e^- \quad (8)$$

$$FeOH^+ = Fe^{+2} + OH^- \quad (9)$$

In both mechanisms, the second step is considered as the rate-determining step and the first and the third steps are postulated to be in pseudo-equilibrium. On the basis of polarization experiments, Lorenz observed both sets of kinetic parameters depending upon the crystal imperfections of the electrode materials (Choi & Kim 2000).

Temperature influence and activation parameters

The influence of temperature range (20–50 °C) on the value of the limiting current, which determines the steel electro-polishing rate, and (IE%) was studied in the absence and presence of different concentrations of the studied polysaccharides extract as shown in Table 3. Results obtained indicate that I_L increases with increasing temperature for different concentrations of tested polysaccharides, with a consequent increase in the rate of electro-polishing process of iron, while IE% decreases with temperature increase (Abdel Rahman *et al.* 2015). This increase in I_L may be attributed to the fact that as the temperature increases, the solution viscosity decreases; hence the diffusivity (D) of Fe^{2+} increases, which leads to increase in I_L and the electro-polishing rate (Abdel Rahman *et al.* 2015).

The retardation in IE% with increase in temperature relates to the fact that raising the temperature of the system lowers the surface coverage of metal surface by inhibitor; therefore the inhibiting effect decreases, which leads to desorption (Akalezi *et al.* 2012; Abouzeid 2016).

Activation parameters of electrochemical polishing process are very useful for understanding the adsorption inhibitor mechanism on metal surface (Abouzeid 2016). The data of activation energy (E_a), and changes in enthalpy ΔH^*, entropy ΔS^* and free energy ΔG^* of activation for steel anodic polishing process in absence and presence of the studied blue inhibitor were calculated by the following equations and are presented in Table 4.

E_a is estimated by linear integrated form of the Arrhenius equation:

$$\ln I_L = \ln A - E_a/RT \quad (10)$$

Plotting of $\ln I_l$ versus 1/T gives a straight line with slope equal to $-E_a/R$, from which E_a can be calculated, Figure 10.

ΔH^*, ΔS^* and ΔG^* are determined by the activation state equation:

$$I_L = (RT/Nh)\exp(\Delta S^*/R)\exp(-\Delta H^*/RT) \quad (11)$$

$$\Delta G^* = \Delta H^* - T\Delta S^* \quad (12)$$

where I_L is the limiting current obtained from the polarization curves, A is the Arrhenius pre-exponential factor, R

Table 4 | Activation energy and activation parameters in absence and presence of 20 ppm of different polysaccharides at 8 M H_3PO_4

Compounds	ΔH^* (kJ mol^{-1})	$-\Delta S^*$ (J mol^{-1} K^{-1})	ΔG^* (kJ mol^{-1})	E_a (kJ mol^{-1})
Blank	4.97	234.26	68.64	7.53
Alginate	5.34	233.38	68.39	7.90
Crude polysaccharide	5.93	231.77	67.92	8.49
Fucoidan	6.41	230.48	67.54	8.97

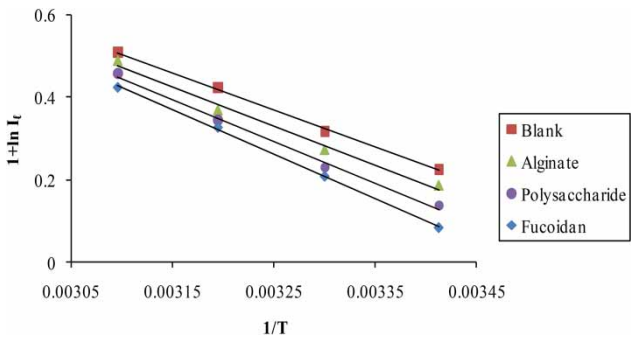

Figure 10 | The Arrhenius plot of the electro-polishing process for steel electrode in 8 M H_3PO_4 in absence and presence of different polysaccharide.

is the universal gas constant, T is the absolute temperature, N is Avogadro's number and h is Plank's constant.

The plot of ln (I_L/T) against 1/T gives a straight line with slope of $-\Delta H^*/R$ and intercept ln $(R/Nh) + \Delta S^*/R$ (Figure 11) from which the values of ΔS^* and ΔH^* were evaluated.

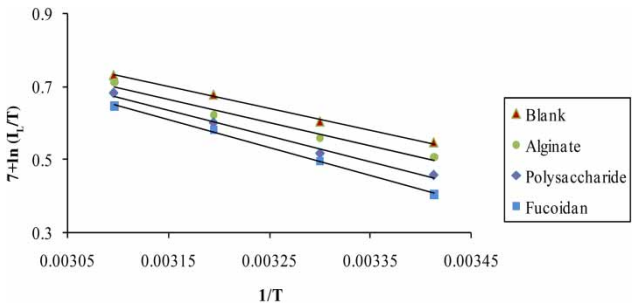

Figure 11 | Plots of ln (I_L/T) versus 1/T for steel electro-polishing in 8 M H_3PO_4 in absence and presence of different polysaccharide.

From Table 4 it is seen that the values of E_a are higher in the presence of fucoidan, crude polysaccharide and alginate than that of the blank indicating that the steel electro-polishing is inhibited by these compounds via formation of electrostatic film during the phenomenon of physical adsorption (Popova *et al.* 2003). Also, E_a value follows the order fucoidan > polysaccharide > alginate > blank, which indicates that fucoidan is a greater inhibitor that retarded anodic polishing through creating a physical barrier to charge and mass transfer of ions via an adsorption mechanism (Taha *et al.* 2020).

The higher values of ΔH^* in presence of extracted inhibitor than the value for blank solution reveals that these additives enhance the height energy barrier of the carbon steel electro-polishing reaction (Popova *et al.* 2003).

The large and negative values of ΔS^* in the absence and presence of additive inhibitor pointed to a greater order produced during the process of activation. This can be explained by the formation of an activated complex in the

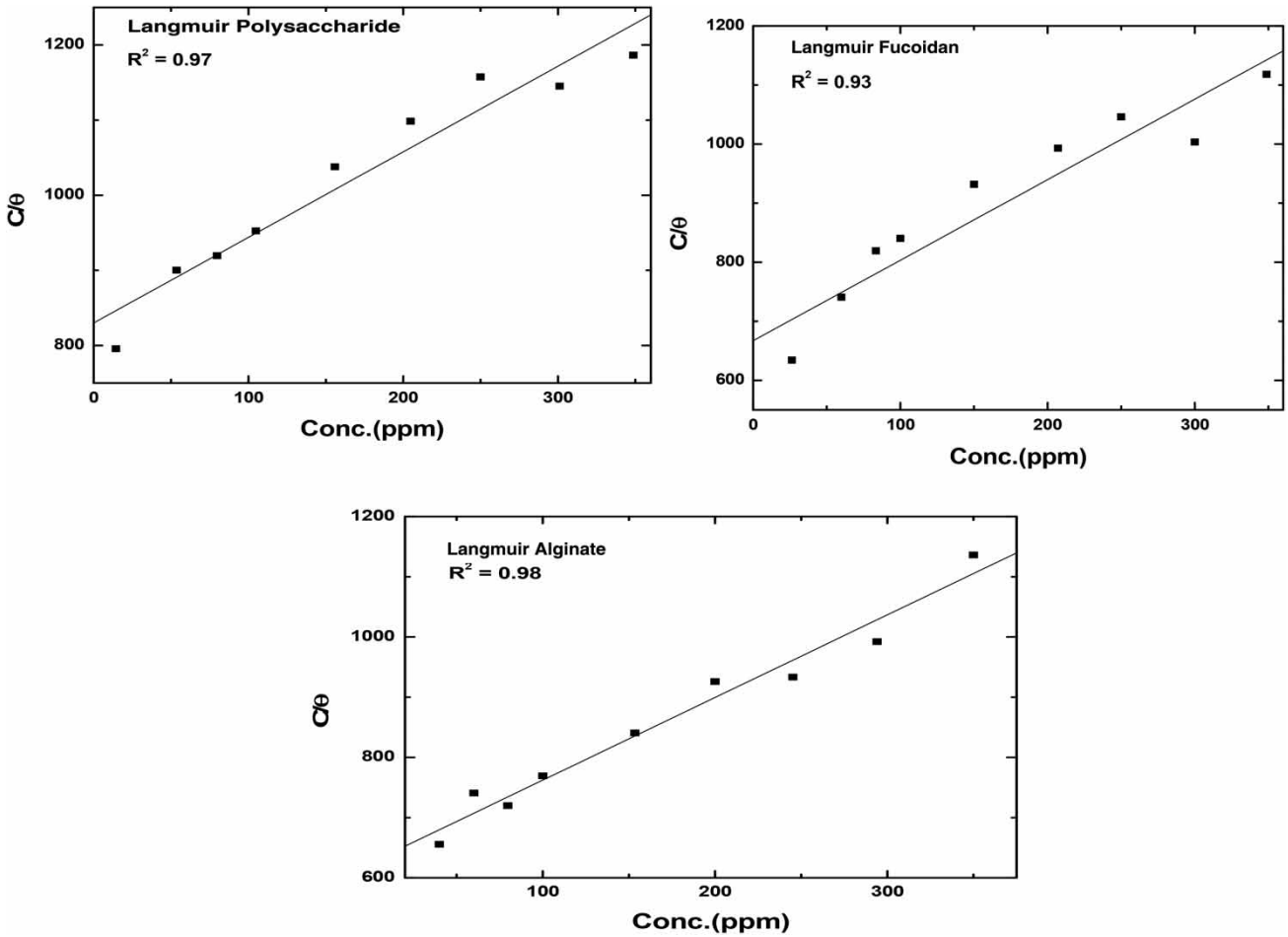

Figure 12 | Langmuir isotherm for crude polysaccharide, fucoidan and alginate at 8 M H_3PO_4 and 20 °C.

rate-determining step which represents fixation with consequent loss in the degrees of freedom of the system during the process (Taha *et al.* 2013a, 2013b).

The ΔG* values in absence and presence of these additives are attributed largely to the general linear compensation between ΔH* and ΔS* for the given temperature and not dependence on composition of these compounds (Abouzeid & Abubshait 2020).

Adsorption isotherms

Adsorption isotherms give information about the interaction among adsorbed molecules themselves as well as their interactions with the metal surface. Surface coverage (θ) values were evaluated from the gravimetric measurements assuming a direct relationship between inhibition efficiency and surface coverage. The surface coverage values (defined as IE%/100) were fitted to different adsorption isotherm models, and the best results judged by the correlation coefficient (R^2) were obtained with the Langmuir isotherm. According to this isotherm the surface coverage is related to concentration inhibitor via this equation (Khadraoui *et al.* 2014):

$$\text{Langmuir: } C/\theta = 1/K + C \tag{13}$$

where C is the concentration of blue inhibitor; K is the equilibrium constant of adsorption process.

It is noticed from Figure 12 that the relation between C/θ and C yielded straight lines for crude polysaccharide, fucoidan and alginate with a very good correlation coefficient (0.97, 0.93 and 0.98) and slopes (1.13, 1.33 and 1.32) respectively. This result indicates that the adsorption of compounds under consideration on the metal–phosphoric acid

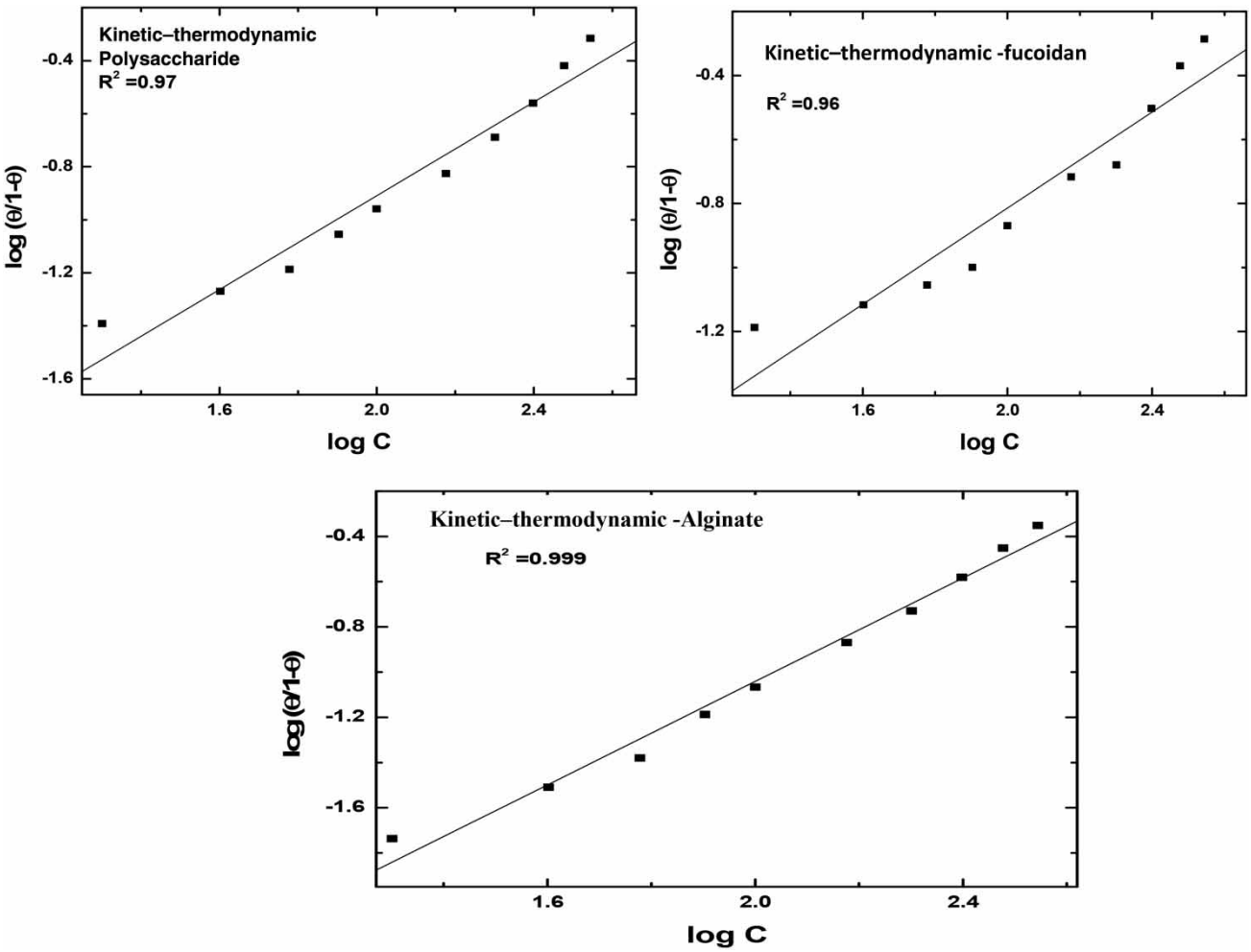

Figure 13 | Kinetic–thermodynamic model for polysaccharide, fucoidan and alginate at 8 M H_3PO_4 and 20 °C.

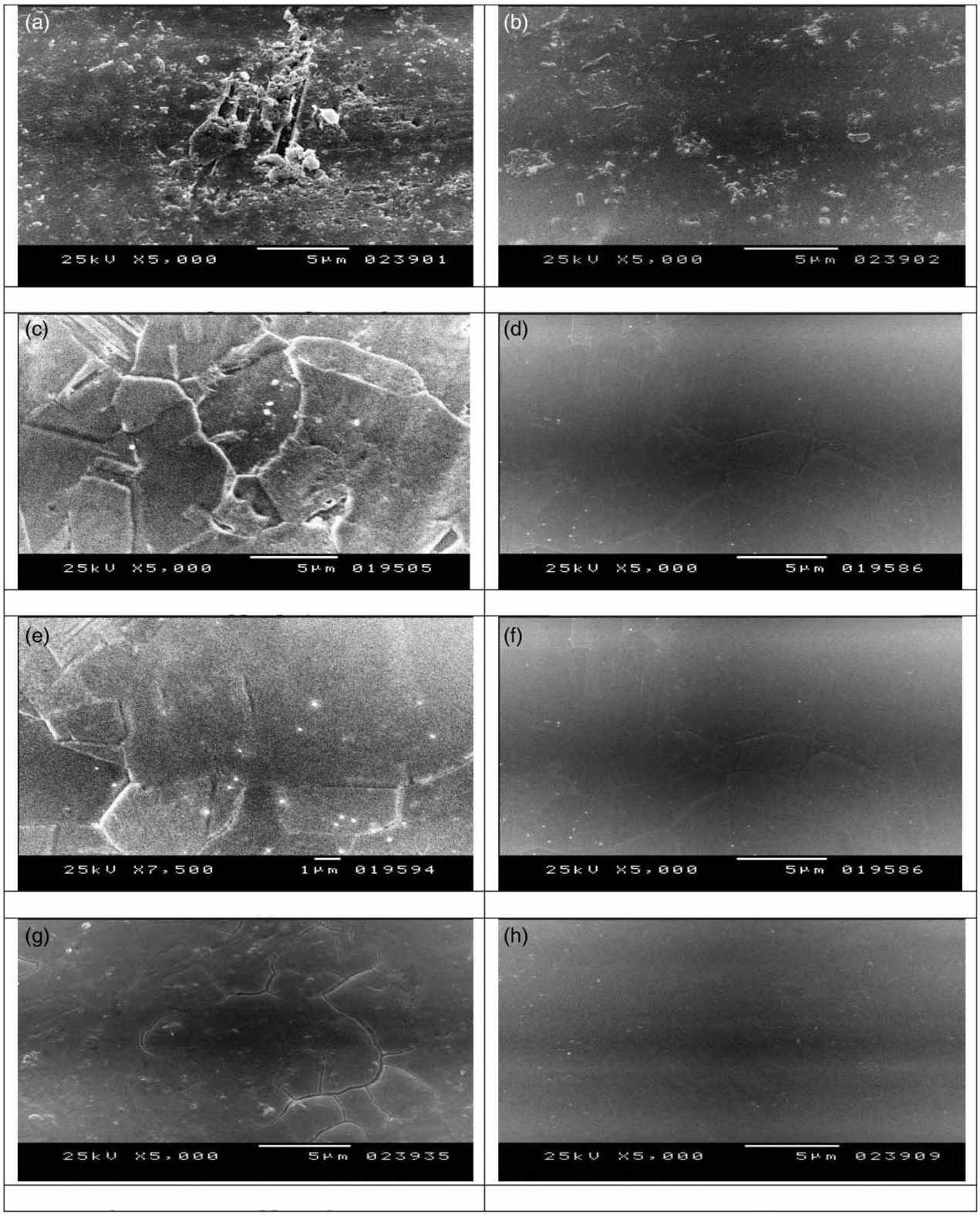

Figure 14 | SEM before and after electro-polishing in the absence and in presence of different concentrations of crude polysaccharide, fucoidan and alginate extract. (a) Raw sample before polishing. (b) After electro-polishing without addition (blank). (c) After electro-polishing + 40 ppm polysaccharide. (d) After electro-polishing + 350 ppm polysaccharide. (e) After electro-polishing + 40 ppm fucoidan. (f) After electro-polishing + 350 ppm fucoidan. (g) After electro-polishing + 40 ppm alginate. (h) After electro-polishing + 350 ppm alginate.

medium interface follows the Langmuir adsorption isotherm. The variations of surface coverage with concentration of extracts are shown in Figure 12. These curves represent adsorption isotherms that are characterized by first sharp rising part followed by another gradual rising part indicating formation of a mono-layer adsorbate film on the steel surface (Taha *et al.* 2013a, 2013b).

The kinetic–thermodynamic model is given by:

$$K(C)^{y} = (\theta/1-\theta) \quad (14)$$

Figure 13 shows the linear fitting of extracts results according to kinetic–thermodynamic model. The y value indicates the number of molecules occupying one active site. The increase of y value in the presence of crude polysaccharide, fucoidan and alginate in medium (0.94, 0.88 and 1.14) indicates that a larger number of extracted molecules occupy one active site and this behavior confirmed the result obtained from Langmuir (Taha *et al.* 2013a, 2013b).

Scanning electron microscopy (SEM)

SEM was used to investigate the surface morphology of the steel sheet in 8 M H_3PO_4 at 20 °C. Micrographs of the specimens before and after electro-polishing in the absence and in the presence of different concentrations of polysaccharide, fucoidan and alginate extract under investigation are shown in Figure 14.

An uneven and damaged surface and also large deep pits are clearly seen in the raw sample, Figure 14(a). After electro-polishing in 8 M H_3PO_4, the surface texture was enhanced to some extent, Figure 14(b) (Taha *et al.* 2013a, 2013b).

After addition of low concentration (40 ppm) of polysaccharide, fucoidan and alginate extract (Figure 14(c), 14(e) and 14(g)) it is observed that grain boundaries are the most common shape represented on the sample, and deep cavities were also found, but after the addition of high concentration (350 ppm) of polysaccharide, fucoidan and alginate extract Figure 14(d), 14(f) and 14(h) grain boundaries are also shown but the surface appears more uniform and smooth and improvement of the surface texture takes place which may be attributed to adsorption of polysaccharide, fucoidan and alginate on steel surface; high viscosity of extracts decrease the aggressive attack of acid for steel sheet and presence of a high density of OH groups retarded randomness of anodic electro-polishing of steel (Abdel Rahman *et al.* 2015).

CONCLUSIONS

- Extracts of different polysaccharides (crude polysaccharide, fucoidan and alginate) under investigation were used as a blue inhibitor for electro-polishing of anodic carbon steel.
- IE% increases as the concentrations of all these polysaccharides increase, and the electro-polishing process of steel is decreased consequently.
- Fucoidan is more inhibitory than the other extracts owing to the chemical composition of fucoidan (negatively charged poly center sites due to high sulfate content) being different from the other compounds, which was proved by FT-IR and value of E_a.
- Mechanism of anodic steel electro-polishing in presence of previous additives followed physical adsorption, which was confirmed by the activation energy values.
- The adsorption of these extracts onto steel sheet obeyed Langmuir and kinetic adsorption models.
- Finally, steel surface at high concentrations of different polysaccharides during anodic polishing became more smooth and bright, which was confirmed by SEM, suggesting that blue sorption inhibitors were present on the steel metal.

DATA AVAILABILITY STATEMENT

All relevant data are available from an online repository or repositories: http://researchdata.4tu.nl/en/home/.

REFERENCES

Abdel Rahman, H. H., Seleim, M. S., Hafez, A. M. & Helmy, A. A. 2015 Study of electropolishing inhibition of steel using natural products as a green inhibitor in ortho-phosphoric acid. *Green Chemistry Letters and Reviews* **8**, 88–94.

Abouzeid, F. M. 2016 Comparison between electropolishing behavior of copper and mild steel in the presence of lactic and mandolic acid. *International Journal of Electrochemical Science* **11**, 7269–7281.

Abouzeid, F. M. & Abubshait, H. A. 2020 A study of vitamin B influence on the morphology, roughness, and reflectance of electropolished aluminum in H_3PO_4-H_2SO_4 mixture. *Arabian Journal of Chemistry* **13**, 2579–2595.

Akalezi, C. O., Enenebaku, C. K. & Oguzie, E. E. 2012 Application of aqueous extracts of coffee senna for control of mild steel corrosion in acidic environments. *International Journal of Industrial Chemistry* **3**, 13–25.

Ale, M. T., Mikkelsen, J. D. & Meyer, A. 2011 Important determinants for fucoidan bioactivity: a critical review of structure-function relations and extraction methods for fucose-containing sulfated polysaccharides from brown seaweeds. *Marine Drugs* **9**, 2106–2130.

Allam, A. M., Ateya, B. G. & Pickering, H. W. 1997 Effect of chloride ions on adsorption and permeation of hydrogen in iron. *Corrosion* **53**, 284–289.

AOAC 1990 *Official Methods of Analysis*, 15th edn. Association of Official Analytical Chemists, Arlington, VA, USA.

AOAC 2000 *Official Methods of Analysis*, 16th edn. Association of official Analytical Chemists, Arlington, VA, USA.

APHA, AWWA & WEF 1999 *Standard Methods for the Examination of Water and Wastewater*, 20th edn. American Public Health Association/American Water Works Association/Water Environment Federation, Washington DC, USA.

Awad, A. M., Abdel Ghany, N. A. & Dahy, T. M. 2010 Removal of tarnishing and roughness of copper surface by electropolishing treatment. *Journal of Applied Surface Science* **256**, 4370–4375.

Benabbouha, T., Siniti, M., El Attari, H., Chefira, K., Chibi, F., Nmila, R. & Rchid, H. 2018 Red algae *Halopitys incurvus* extract as a green corrosion inhibitor of carbon steel in hydrochloric acid. *Journal of Bio- and Tribo-Corrosion* **4**, 39–44.

Benabbouha, T., Siniti, M., El Attari, H., Chefira, K., Chibi, F., Nmila, R. & Rchid, H. 2020 The brown algae *Cystoseira baccata* extract as a friendly corrosion inhibitor on carbon steel in acidic media. *SN Applied Sciences* **2**, 662–671.

Berteau, O. & Mulloy, B. 2003 Sulfated fucans, fresh perspectives: Structures, functions, and biological properties of sulfated fucans, and an overview of enzymes active toward this class of polysaccharide. *Glycobiology* **13**, 29–40.

Besednova, N. N., Zaporozhets, S., Makarenkova, I. D., Kuznetsova, T. A., Kryzhanoskii, S. P., Bilan, M. I., Grachev, A. A., Shashkov, A. S., Kelly, M., Sanderson, C. J. & Nifantiev, N. E. 2010 Further studies on the composition and structure of a fucoidan preparation from the brown alga *Saccharina latissima*. *Carbohydrate Research* **345**, 2038–2047.

Bilan, M. I., Grachev, A. A., Shashkov, A. S., Kelly, M., Sanderson, C. J. & Nifantiev, N. E. 2010 Further studies on the composition and structure of a fucoidan preparation from the brown alga *Saccharina latissima*. *Carbohydrate Research* **345**, 2038–2047.

Bockris, J. M. & Reddy, A. K. N. 2002 *Modern Electrochemistry-Ionics*, Vol. 1. Springer Science+Business Media, New York, USA, p. 1232

Campos-Vallette, M. M., Chandía, N. P., Clavijo, E., Leal, D., Matsuhiro, B., Osorio-Román, I. O. & Torres, S. 2010 Characterization of sodium alginate and its block fractions by surface-enhanced Raman spectroscopy. *Journal of Raman Spectroscopy* **41**, 758–763.

Chandía, N. P. & Matsuhiro, B. 2008 Characterization of a fucoidan from *Lessonia vadosa* (Phaeophyta) and its anticoagulant and elicitor properties. *International Journal of Biological Macromolecules* **42**, 235–240.

Choi, Y. S. & Kim, J. G. 2000 Aqueous corrosion behavior of weathering steel and carbon steel in acid-chloride environments. *Corrosion* **56**, 1202–1210.

Draget, K. I., Moe, S. T., Skjåk-Bræk, G. & Smidsrød, O. 2006 Alginates. In: *Food Polysaccharides and their Applications*, Vol. 14 (A. M. Stephen, G. O. Phillips & P. A. Williams, eds). CRC Press, Boca Raton, FL, USA, pp. 159–1178

El-Rafie, H. M., El-Rafie, M. H. & Zahran, M. K. 2013 Green synthesis of silver nanoparticles using polysaccharides extracted from marine macro algae. *Carbohydrate Polymers* **96**, 403–410.

Fletcher, H. R., Biller, P., Ross, A. B. & Adams, J. M. M. 2017 The seasonal variation of fucoidan within three species of brown macroalgae. *Algal Research* **22**, 79–86.

Guiry, M. D. & Guiry, G. M. 2019 *Algae Base*. World-wide electronic publication, National University of Ireland, Galway, Ireland.

Hassan, H. H. 2007 Inhibition of mild steel corrosion in hydrochloric acid solution by triazole derivatives: Part II: Time and temperature effects and thermodynamic treatments. *Electrochimica Acta* **53**, 1730.

Haug, A., Melsom, S. & Omang, S. 1974 Estimation of heavy metal pollution in two Norwegian fjord areas by analysis of the brown alga *Ascophyllum nodosum*. *Environmental Pollution* **7**, 179–192.

Ismail, M. M., El Zokm, G. M. & El-Sayed, A. A. M. 2017 Variation in biochemical constituents and master elements in common seaweeds from Alexandria Coast, Egypt with special reference to their antioxidant activity and potential food uses: prospective equations. *Environmental Monitoring and Assessment* **189**, 648–665.

Jayaraman, J. D., Sigamani, S., Venkatachalam, H. & Ramamurthy, D. 2016 Extraction and purification of sulfated polysaccharide from brown algae and its efficacy in preventing blood clotting. *Asian J. Biol. Life Sci.* **5** (3), 237–244.

Kanaan, H. & Belous, O. 2016 *Marine Algae of the Lebanese Coast*. Nova science publisher, Inc, New York, USA.

Kannan, S. 2014 FT-IR and EDS analysis of the seaweeds *Sargassum wightii* (brown algae) and *Gracilaria corticata* (red algae). *International Journal of Current Microbiology and Applied Science* **3**, 341–351.

Khadraoui, A., Khelifa, A., Boutoumi, H., Hamitouche, H., Mehdaoui, R., Hammouti, B. & Al-Deyab, S. S. 2014 Adsorption and inhibitive properties of *Ruta chalepensis* L. oil as a green inhibitor of steel in 1M hydrochloric acid medium. *International Journal of Electrochemical Science* **9**, 3334–3338.

Kim, K.-T. 2012 *Seasonal Variation of Seaweed Components and Novel Biological Function of Fucoidan Extracted from Brown Algae in Quebec*. PhD Thesis, Université Laval.

Kim, H. S., Lee, C.-G. & Lee, E. Y. 2011 Alginate lyase: structure, properties. *Engineering* **16**, 843–851.

Kimura, T., Ueda, K., Kuroda, R., Akao, T., Shinohara, N., Ushirokawa, T., Fukagawa, A. & Akimoto, T. 2007 The seasonal variation in polysaccharide content of brown alga akamoku*Sargassum horneri* collected off Oshima Island (Fukuoka Prefecture). *Nippon Suisan Gakkaishi* **73** (4), 739–744.

Kloareg, B., Demarty, M. & Mabeau, S. 1986 Polyanionic characteristics of purified sulphated homofucans from brown algae. *International Journal of Biological Macromolecules* **8**, 380–386.

Larsen, B., Salem, D. M. S. A., Sallam, M. A. E., Mishrikey, M. M. & Beltagy, A. I. 2003 Chemical, physical and biological properties of alginates and their biomedical implications. *Carbohydrate Research* **338**, 2325–2336.

Lim, S. J., Aida, W. M. W., Maskat, M. Y., Mamot, S., Ropien, J. & Mohd, D. M. 2014 Isolation and antioxidant capacity of fucoidan from selected Malaysian seaweeds. *Food Hydrocolloids* **42**, 280–288.

Mestechkina, N. M. & Shcherbukhin, V. D. 2010 Sulfated polysaccharides and their anticoagulant activity: a review. *Applied Biochemistry and Microbiology* **46**, 291–298.

Nakamoto, K. 1986 *Infrared and Raman Spectra of Inorganic and Coordination Compounds*. Wiley, New York, USA.

Nancy, P. C., Betty, M., Enrique, M. & Alejandra, M. 2004 Alginic acids in *Lessonia vadosa*: partial hydrolysis and elicitor properties of the polymannuronic acid fraction. *Journal of Applied Phycology* **16**, 127–133.

Paniagua-Michel, J., Olmos-Soto, J. & Morales-Guerrer, E. R. 2014 Chapter eleven – algal and microbial exopolysaccharides: new insights as biosurfactants and bioemulsifiers. *Advances in Food and Nutrition Research* **73**, 221–257.

Pereira, L., Sousa, A., Coelho, H., Amado, M. A. & Ribeiro-Calro, A. J. P. 2003 Use of FT-IR, FT-Raman and 13-C NMR spectroscopy for identification of some seaweed phycocolloids. *Biomolecular Engineering* **20**, 223–228.

Popova, A., Sokolova, E., Raicheva, S. & Christov, M. 2003 AC and DC study of the temperature effect on mild steel corrosion in acid media in the presence of benzimidazole derivatives. *Corrosion Science* **45**, 33–58.

Preeprame, S., Hayashi, K., Lee, J. B., Sankawa, U. & Hayashi, T. 2001 A novel antivirally active fucan sulfate derived from and edible brown alga *Sargassum horneri*. *Chemical and Pharmaceutical Bulletin* **49**, 484–485.

Ramdani, M., Elmsellem, H., Elkhiati, N., Haloui, B., Aouniti, A., Ramdani, M., Ghazi, Z., Chetouani, A. & Hammouti, B. 2015 *Caulerpa prolifera* green algae using as eco-friendly corrosion inhibitor for mild steel in 1 M HCl media. *Der Pharma Chemica* **7** (2), 67–76.

Rioux, L. E., Turgeon, S. L. & Beaulieu, M. 2007 Characterization of polysaccharides extracted from brown seaweeds. *Carbohydrate Polymers* **69**, 530–537.

Robinson, H. B. 1958 Method of electropolishing and electrolytic solutions therefore. United States Patent 2,861,930.

Rodríguez-Montesinos, Y. E., Arvizu-Higuera, D. L. & Hernández-Carmona, G. 2008 Seasonal variation on size and chemical constituents of *Sargassum sinicola* Setchell et Gardner from Bahía de La Paz, Baja California Sur, Mexico. *Phycological Research* **56**, 33–38.

Sheng, P. X., Ting, Y.-P., Chen, J. P. & Hong, L. 2004 Sorption of lead, copper, cadmium, zinc, and nickel by marine algal biomass: characterization of biosorptive capacity and investigation of mechanism. *Journal of Colloid and Interface Science* **275**, 131–141.

Silverstein, R. M. & Webster, F. X. 1998 *Spectrometric Identification of Organic Compounds*, 6th edn. John Wiley and Sons, Inc, New York, USA.

Taha, A. A., Abdel Rahman, H. H. & Abouzeid, F. M. 2013a Effect of surfactants on the rate of diffusion controlled anodic dissolution of copper in orthophosphoric acid. *International Journal of Electrochemical Science.* **8**, 6744–6762.

Taha, A. A., Abdel Rahman, H. H. & Abouzeid, F. M. 2013b Study of factors influencing on dissolution behavior of copper in orthophosphoric acid using rotating cylinder electrode (RCE) and rotating disc electrode (RDE). *International Journal of Electrochemical Science* **8**, 9041–9059.

Taha, A. A., Abouzeid, F. M. & Kandil, M. M. 2020 Some drugs effect on the electropolishing of C-steel in H_3PO_4 acid under normal and compulsory convection circumstances. *Russian Journal of Electrochemistry* **56**, 189–205.

Verma, D. K. & Khan, F. 2016 Green approach to corrosion inhibition of mild steel in hydrochloric acid medium using extract of spirogyra algae. *Green Chemistry Letters and Reviews* **9** (1), 52–60.

Vracar, L. j. & Drazic, D. M. 1992 Influence of chloride ion adsorption on hydrogen evolution reaction on iron. *Journal of Electroanalytical Chemistry* **339**, 269–279.

Wang, Y., Xing, M., Cao, Q., Ji, A., Liang, H. & Song, S. 2019 Biological activities of fucoidan and the factors mediating its therapeutic effects: a review of recent studies. *Marine Drugs* **17**, 1–18.

Zhao, Y., Zheng, Y. Z., Wang, J., Ma, S. Y., Yu, Y. M. & White, W. L. 2018 Fucoidan extracted from *Undaria pinnatifida*: source for nutraceuticals/functional foods. *Marine Drugs* **16**, 321–338.

Zou, P., Lu, X., Zhao, H., Yuan, Y., Meng, L., Zhang, C. & Li, Y. 2019 Polysaccharides derived from the brown algae *Lessonia nigrescens* enhance salt stress tolerance to wheat seedlings by enhancing the antioxidant system and modulating intracellular ion concentration. *Frontiers in Plant Science* **10**, 1–15.

Zvyagintseva, T. N. & Mel'nikov, V. G. 2012 Anti-inflammatory effects of sulphated polysaccharides extracted from brown marine algae. *Biology Bulletin Reviews* **2**, 525–532.

First received 17 August 2020; accepted in revised form 23 November 2020. Available online 8 December 2020